Manuscript Details

Manuscript number	JPSYCHIATRRES_2019_651_R2
Title	Schizophrenia polygenic risk score influence on white matter microstructure
Article type	Short Communication

Abstract

Schizophrenia (SZ) and bipolar disorder (BD) are highly heritable, share symptomatology, and have a polygenic architecture. The impact of recent polygenic risk scores (PRS) for psychosis, which combine multiple genome-wide associated risk variations, should be assessed on heritable brain phenotypes also previously associated with the illnesses, for a better understanding of the pathways to disease. We have recently reported on the current SZ PRS's ability to predict 1st episode of psychosis case-control status and general cognition. Herein, we test its penetrance on white matter (WM) microstructure, which is known to be impaired in SZ, in BD and their relatives, using 141 participants (including SZ, BP, relatives of SZ or BP patients, and healthy volunteers), and two WM integrity indexes: fractional anisotropy (FA) and mean diffusivity (MD). No significant correlation between the SZ PRS and FA or MD was found, thus it remains unclear whether white matter changes are primarily associated with SZ genetic risk profiles.

Keywords	polygenic risk score, PRS, schizophrenia, bipolar disorder, white matter, diffusion tensor imaging, psychosis, fractional anisotropy, mean diffusivity, GWA, genome-wide association
Taxonomy	Schizophrenia, Genetics, Brain Imaging
Manuscript region of origin	Europe

Corresponding Author	Diana Prata
Corresponding Author's Institution	King's College London
Order of Authors	Beatriz SImoes, Evangelos Vassos, sukhi shergill, Colm McDonald, Timothea Toulopoulou, Sridevi Kalidindi, Fergus Kane, Robin Murray, Elvira Bramon, Hugo Ferreira, Diana Prata
Suggested reviewers	Nicholas Stefanis, Stefan Borgwardt, Dan Rujescu, Michael O'Donovan

Submission Files Included in this PDF

File Name [File Type]

Cover letter.docx [Cover Letter]

Cover letter_Revision_BS_10.09.2019_DP_revised.docx [Response to Reviewers]

Abstract.docx [Abstract]

Title Page.docx [Title Page (with Author Details)]

Manuscript Simoes et al_JournalPsychResearch_BS_10.09.2019_DP_revised.docx [Manuscript File]

Conflict of Interest.docx [Conflict of Interest]

Author Statement.docx [Author Statement]

Supplementary_material_2_BS_10.09.2019_DP_revised.docx [e-Component]

To view all the submission files, including those not included in the PDF, click on the manuscript title on your EVISE Homepage, then click 'Download zip file'.

Research Data Related to this Submission

There are no linked research data sets for this submission. The following reason is given:
Data will be made available on request

Abstract

Schizophrenia (SZ) and bipolar disorder (BD) are highly heritable, share symptomatology, and have a polygenic architecture. The impact of recent polygenic risk scores (PRS) for psychosis, which combine multiple genome-wide associated risk variations, should be assessed on heritable brain phenotypes also previously associated with the illnesses, for a better understanding of the pathways to disease. We have recently reported on the current SZ PRS's ability to predict 1st episode of psychosis case-control status and general cognition. Herein, we test its penetrance on white matter microstructure, which is known to be impaired in SZ, in BD and their relatives, using 141 participants (including SZ, BP, relatives of SZ or BP patients, and healthy volunteers), and two white matter integrity indexes: fractional anisotropy (FA) and mean diffusivity (MD). No significant correlation between the SZ PRS and FA or MD was found, thus it remains unclear whether white matter changes are primarily associated with SZ genetic risk profiles.

Schizophrenia polygenic risk score influence on white matter microstructure

Beatriz Simões[1], Msc, Evangelos Vassos[2], PhD, Sukhi Shergill[3], PhD, Colm McDonald[4], PhD, Timothea Toulopoulou[3,6,7], PhD, Sridevi Kalidindi[3,8], PhD, Fergus Kane[3], PhD, Robin Murray[3], PhD, Elvira Bramon[3,9], PhD, Hugo Ferreira[1], PhD Diana Prata[1,10,11], PhD

[1]Instituto de Biofísica e Engenharia Biomédica, Faculdade de Ciências, Universidade de Lisboa, Portugal

[2]Social, Genetic and Developmental Psychiatry Centre, Institute of Psychiatry, Psychology and Neuroscience, King's College London, UK

[3]Department of Psychosis Studies, Institute of Psychiatry, Psychology & Neuroscience, King's College London, London, UK

[4]Centre for Neuroimaging & Cognitive Genomics (NICOG), NCBES Galway Neuroscience Centre, National University of Ireland Galway, Ireland.

[6]Department of Psychology, The University of Hong Kong, Hong Kong Special Administrative Region

[7]Department of Psychology, Bilkent University, Turkey

[8]South London and Maudsley NHS Foundation Trust, London, UK

[9]Mental Health Neurosciences Research Department, Division of Psychiatry, University College London, London, UK

[10]Department of Neuroimaging, Institute of Psychiatry, Psychology & Neuroscience, King's College London, London, UK

[11]Instituto Universitário de Lisboa (ISCTE-IUL), Centro de Investigação e Intervenção Social, Lisboa, Portugal

Corresponding author: Diana Prata, diana.prata@kcl.ac.uk; Instituto de Biofísica e Engenharia Biomédica, Faculdade de Ciências, Universidade de Lisboa, Campo Grande 016, 1749-016 Lisboa, Portugal

Abstract

Schizophrenia (SZ) and bipolar disorder (BD) are highly heritable, share symptomatology, and have a polygenic architecture. The impact of recent polygenic risk scores (PRS) for psychosis, which combine multiple genome-wide associated risk variations, should be assessed on heritable brain phenotypes also previously associated with the illnesses, for a better understanding of the pathways to disease. We have recently reported on the current SZ PRS's ability to predict 1st episode of psychosis case-control status and general cognition. Herein, we test its penetrance on white matter (WM) microstructure, which is known to be impaired in SZ, in BD and their relatives, using 141 participants (including SZ, BP, relatives of SZ or BP patients, and healthy volunteers), and two WM integrity indexes: fractional anisotropy (FA) and mean diffusivity (MD). No significant correlation between the SZ PRS and FA or MD was found, thus it remains unclear whether white matter changes are primarily associated with SZ genetic risk profiles.

Keywords: polygenic risk score, PRS, schizophrenia, bipolar disorder, white matter, diffusion tensor imaging, psychosis, fractional anisotropy, mean diffusivity, GWA, genome-wide association

Schizophrenia polygenic risk score influence on white matter microstructure

Beatriz Simões[1], Msc, Evangelos Vassos[2], PhD, Sukhi Shergill[3], PhD, Colm McDonald[4], PhD, Timothea Toulopoulou[3,6,7], PhD, Sridevi Kalidindi[3,8], PhD, Fergus Kane[3], PhD, Robin Murray[3], PhD, Elvira Bramon[3,9], PhD, Hugo Ferreira[1], PhD, Diana Prata[1,10,11], PhD

[1]Instituto de Biofísica e Engenharia Biomédica, Faculdade de Ciências, Universidade de Lisboa, Portugal

[2]Social, Genetic and Developmental Psychiatry Centre, Institute of Psychiatry, Psychology and Neuroscience, King's College London, UK

[3]Department of Psychosis Studies, Institute of Psychiatry, Psychology & Neuroscience, King's College London, London, UK

[4]Centre for Neuroimaging & Cognitive Genomics (NICOG), NCBES Galway Neuroscience Centre, National University of Ireland Galway, Ireland.

[6]Department of Psychology, The University of Hong Kong, Hong Kong Special Administrative Region

[7]Department of Psychology, Bilkent University, Turkey

[8]South London and Maudsley NHS Foundation Trust, London, UK

[9]Mental Health Neurosciences Research Department, Division of Psychiatry, University College London, London, UK

[10]Department of Neuroimaging, Institute of Psychiatry, Psychology & Neuroscience, King's College London, London, UK

[11]Instituto Universitário de Lisboa (ISCTE-IUL), Centro de Investigação e Intervenção Social, Lisboa, Portugal

Corresponding author: Diana Prata, diana.prata@kcl.ac.uk; Instituto de Biofísica e Engenharia Biomédica, Faculdade de Ciências, Universidade de Lisboa, Campo Grande 016, 1749-016 Lisboa, Portugal

Abstract

Schizophrenia (SZ) and bipolar disorder (BD) are highly heritable, share symptomatology, and have a polygenic architecture. The impact of recent polygenic risk scores (PRS) for psychosis, which combine multiple genome-wide associated risk variations, should be assessed on heritable brain phenotypes also previously associated with the illnesses, for a better understanding of the pathways to disease. We have recently reported on the current SZ PRS's ability to predict 1st episode of psychosis case-control status and general cognition. Herein, we test its penetrance on white matter microstructure, which is known to be impaired in SZ, in BD and their relatives, using 141 participants (including SZ, BP, relatives of SZ or BP patients, and healthy volunteers), and two white matter integrity indexes: fractional anisotropy (FA) and mean diffusivity (MD). No significant correlation between the SZ PRS and FA or MD was found, thus it remains unclear whether white matter changes are primarily associated with SZ genetic risk profiles.

Keywords: polygenic risk score, PRS, schizophrenia, bipolar disorder, white matter, diffusion tensor imaging, psychosis, fractional anisotropy, mean diffusivity, GWA, genome-wide association

INTRODUCTION

Schizophrenia (SZ) and bipolar disorder (BD) overlap in symptomatology, are both highly heritable, share genetic susceptibility, and their etiology is still little understood (Craddock and Owen, 2005). In a standard genome-wide association approach (GWAs), the SZ Psychiatric Genomic Consortium-2 (PGC2) meta-analysis found 108 genetic variants to be independently associated with SZ (Ripke et al., 2014), each showing a 1-2 odds ratio. Complementarily, one can examine disorder prediction by summarizing variation across all the associated at various levels of significance loci into a quantitative score, i.e. a polygenic risk score (PRS) (Ripke et al., 2014). Using this approach, we have recently reported the PGC2-SZ PRS to explain 9.2% of SZ case-control variance in a sample of first episode psychosis (Vassos et al., 2017) and 2.7% of general cognitive ability (Toulopoulou et al., 2019).

Reduced fractional anisotropy (FA) and increased mean diffusivity (MD) in white matter, with heritability ranging 30-82%, except in the fornix where it is untypically low (Vuoksimaa et al., 2017), have consistently been reported in SZ and, to a lesser extent, in BD patients, in studies employing Tract Based Spatial Statistics (TBSS) (Ambrosi et al., 2013; Hummer et al., 2016; Kanaan et al., 2017; Subramaniam et al., 2017; Viher et al., 2016; Zhuo et al., 2016). While a unipolar depression PRS has been negatively associated with FA (a proxy for white matter microstructure integrity) in depression and health (N=132) (Whalley et al., 2013), no association was found between SZ, a BD or a unipolar SZ PRSs and white matter microstructure, in a study using the UK Biobank data (N=816) (Reus et al., 2017). However, the UK Biobank study, although powerful, has mixed patients of indiscriminate types, healthy individuals and those without clinical records, which prevented the examination of diagnosis by PRS interactions on brain structure, or a safeguard against noise or confounder effects.

In the present study, we aimed to test the effect of the PGC2-SZ PRS on white matter microstructure integrity, using FA and MD as proxies, in healthy individuals, SZ, BD and SZ/BD relatives' (REL) samples. Considering that both a high SZ PRS (Ruderfer et al., 2014; Tesli et al., 2014) a decreased FA (Ambrosi et al., 2013; Hummer et al., 2016; Kanaan et al., 2017; Subramaniam et al., 2017; Viher et al., 2016; Zhuo et al., 2016), and an increased MD, (Kanaan et al., 2017; Squarcina et al., 2017; Zhuo et al., 2016), are associated with SZ and BD, our main hypothesis was that PGC2-SZ PRS would be negatively associated with FA (and positively with MD). In addition, we also examined whether the effects of PGC2-SZ PRS on FA/MD would be different between the different diagnostic groups, since ours and others previous work, have shown significant genotype by diagnosis effects on these brain measures (Gurung and Prata, 2015; Mallas et al., 2016).

METHODS

DTI and PRS data were selected from a dataset used in previous studies (Allin et al., 2011; Chaddock et al., 2009; Kanaan et al., 2017; Kyriakopoulos et al., 2009; Mallas et al., 2016; Picchioni et al., 2006; Shergill et al., 2007) at the Institute of Psychiatry, Psychology and Neuroscience (IoPPN), King's College London. The selected 141 subjects were divided in four different diagnostic groups: SZ (n=21), BD (n=25), BD/SZ relatives (BD/SZ REL; n=27) and healthy controls (n=68). Demographics statistical tests using IBM SPSS 25 (IBM Corp., 2017) showed BD to be significantly older than healthy individuals (Mann-Whitney U= 528.500, p-value= 0.005); and REL's IQ z-scores to be higher than SZ's (U= 145.500; p-value= 0.004), and higher than healthy individuals (U= 561.000; p-value= 0.003). As expected, PRS was associated with diagnosis (F=4.575, p-value= 0.004; see Figure 1), with PRS being higher in SZ than HC (Tukey's HSD mean difference = 0.844, p -value = 0.003; see Figure 1), but not significantly correlated with any of the demographic variables. Chlorpromazine equivalents (CPZ) were also calculated for the patients groups for descriptive reasons, and for its ascertainment as a confounding factor. As CPZ was not statistically significantly associated with the PRS (Pearson's correlation = 0.169, p-value = 0.441, among both patient groups) in the present sample, nor with white matter microstructure (namely FA) in a largely overlapping sample (Kanaan et al., 2009) (which has later been independently reinforced (Wang et al., 2013)), antipsychotic medication was herein not considered a potential confounding, nor a relevant nuisance, factor. For further demographics statistics, see Supplementary Table 1.

DNA was extracted, processed and genotyped as we previously described (Vassos et al., 2017). The PGC2-SZ PRS was calculated for each participant as the sum of the risk single nucleotide polymorphisms (SNPs) weighted by the logarithm of odds ratio of their respective association with SZ in the PGC2 meta-analysis (Ripke et al., 2014), using the set of statistically significant SNPs with the highest case-control explanatory power which we have previously determined in an independent sample (Vassos et al., 2017).

MRI data was acquired as we previously described (Mallas et al., 2016). Preprocessing of the diffusion MRI images was made using FSL version 5.0.8 (Jenkinson et al., 2012), and included eddy currents distortions correction and brain-extraction with a threshold of 0.2 to ensure a balance between complete scalp removal and inappropriate erosion of brain tissue. FA and MD images were created by fitting a tensor model to the raw diffusion data.

Voxel-wise statistical analysis of FA and MD data was carried out using TBSS (Smith et al., 2006)(Jenkinson et al., 2012) and then fed into a general linear model (GLM) (Smith et al., 2006), both in FSL version 5.0.8. Main effects of PGC2-SZ PRS on FA/MD, followed a regression design (with diagnosis as a covariate of no interest), and PGC2-SZ PRS x diagnosis interaction an ANCOVA, with a permutation-based approach (Smith and Nichols, 2009). Age and gender were added to the models as they showed a predicted significant large effect on FA or MD (namely, corpus callosum ($p = 0.002$), cingulum ($p=0.047$) and superior longitudinal fasciculus ($p=0.049$); and gender on MD in the anterior thalamic radiation ($p=0.049$)).

Statistical significance was considered when effects surpassed the threshold free cluster enhancement (TFCE)-correction at a p-value < 0.05, while trends were considered so when showing a TFCE-uncorrected p-value < 0.01, following standard practice (Mallas et al., 2016; Subramaniam et al., 2017; Viher et al., 2016). The 10 largest clusters of each contrast are reported in Table 1, for conciseness; with the extended list in Supplementary Table 3. For each effect, the R^2 effect size was calculated based on the t-statistics value of the peak voxel (which determines, along with cluster size, the TFCE corrected p-valueLastly, to determine the white matter regions/tracts the Johns Hopkins University ICBM-DTI-81 white-matter label atlas (https://fsl.fmrib.ox.ac.uk/fsl/fslwiki/Atlases) was used. If no region was retrieved, labelling was carried out manually using the MRI Atlas of Human white matter (Mori et al., 2005). Further detail on methods are presented as supplementary information.

RESULTS

Main effect of PGC2-SZ PRS on fractional anisotropy and mean diffusivity

The main effects of PRS on either FA or MD were not statistically significant. However, negative trends were found whereby PRS was correlated with FA in five regions, of which the right cingulum showed the largest cluster, and the only *positive* trend of PRS on FA was found in the anterior thalamic radiation (see Table 1 and Figure 2). On MD, positive trends were seen in four equality small clusters/regions, and one negative trend in the inferior cerebellar peduncle (see Table 1 and Figure 3).

PGC2-SZ PRS x diagnosis interaction on fractional anisotropy and mean diffusivity

No statistically significant PRS x diagnosis interactions on FA or MD were found. Most interactions trends showed similar (small) cluster and effects sizes as the above main effects, except two distinguished by their cluster sizes (albeit their effect sizes explained at maximum of 5% of FA variance): the PRS had a stronger positive correlation with FA on BD than on healthy individuals, and than on SZ: cluster sizes were quite large reaching 3957 voxels in the middle cerebellar peduncle and 1252 in the corticopontine tract, respectively (see Supplementary Table 2).

PRS-FA/MD correlation plots for the peak coordinate of the most TFCE-significant clusters, for each effect described in Table, can be found in Supplementary Figures 1-4.

DISCUSSION

No significant main effects of the PGC2-SZ PRS, or PGC2-SZ PRS by diagnosis interactions, were found on MD or FA. However, both positive and negative TFCE-uncorrected trends (at p-value < 0.01) were found. Main effects, either positive or negative, of PRS on FA were small (in terms of effect size, ranging 0.3–4%). The (expected) negative main effect trends on FA showed one to two orders of magnitude larger cluster sizes reaching 140 voxels in the right cingulum, in comparison with the (unexpected) positive trends (3 voxels). This region's FA shows high heritability (30-70%) (Vuoksimaa et al., 2017) and its white matter alterations have been consistently detected in SZ in previous work (Ellison-Wright and Bullmore, 2009; Knochel et al., 2012; Lener et al., 2015), suggesting it may be implicated in SZ onset. The largest (in terms of effect size) PRS trend on FA was for a negative correlation explaining 4% of variance in the right superior longitudinal fasciculus. Generally one order of magnitude larger than on FA, but still small, were the effects on MD (explaining 4-6% of variance): positive trends were seen in four equally small clusters/regions, and one negative trend in the inferior cerebellar peduncle within a cluster of 12 voxels (see Table 1). Regarding diagnosis-dependent effects of PRS, PRS showed a non-significant higher correlation trend for BD than for healthy individuals or SZ, the clusters being 2-3 orders of magnitude higher than those of the main effects but the effect size being equally small (0.5 - 5%; see Supplementary Table 2).

To put it in perspective, we found the PGC2-SZ PRS to explain a smaller proportion of the variance of FA/MD, than of the observed scale case-control status (9.2%) (Vassos et al., 2017), or than of SZ liability (7%) (Ripke et al., 2014). However its effect magnitude on these brain structure phenotypes was closer to what we found on general cognition (2.7%) (Toulopoulou et al., 2019). This challenges the expectation that penetrance of genetic factors of these complex illnesses on their white matter microstructure or cognitive endophenotypes should be larger than on the illnesses themselves (Iacono, 2018). In the latter cognition study, we have also found more than a quarter of the genetic influence on SZ liability to be mediated through cognition-related paths that were independent of the PRS. Similarly two thirds of the genetic effects on SZ were independent of the PRS (Toulopoulou et al., 2019). Indeed, contrary to the expectations earlier put on endophenotypes, they do not seem to be useful for gene discovery. However, they remain useful for identifying pathways and mechanisms to disease (from gene to brain); and to validate the statistical and clinical usefulness of genetic markers (such as the PRS) previously associated to SZ to predict clinical outcomes (from onset, to diagnosis, prognosis and treatment response). In particular, genetic markers (more than neuroimaging ones) entail the potential to be clinically useful biomarkers due to their screening speed, ease and cost-

effectiveness; even though these are still to be found since our last review on the matter (Prata et al., 2014).

One of the possible reasons for the lack of statistical significance is that our sample size was insufficient to detected an effect, on brain structure, of a PRS which, in its present formula, still explains, albeit robust and well replicated, a small proportion of SZ risk (7-9%) (Ripke et al., 2014; Vassos et al., 2017). Notably, the only other study focusing on the influence of the PGC2-SZ PRS on white matter microstructure (FA/MD), simultaneous to ours, has also not found a significant effect of SZ PRS and FA/MD, even with an approximately 6 times larger sample (Reus et al., 2017), even though that study might (Prata et al., 2014)had other limitations given the highly clinically mixed sample, we did not. However, insufficient power may also arise from the incomplete predictive power of the PGC2 SZ PRS score (which ~7% of the variance in the liability scale currently explained (Ripke et al., 2014)), or, rather, of each of the individual genetic variations reported in the PGC. Given the high heritability of SZ and BD which suggests that genetic factors pose a major contribution to the inherent brain alterations, and the high heritability of some of these well-known brain alterations such as in FA and MD (Vuoksimaa et al., 2017), it is possible that the genetic risk variants that contribute most to the disorders, and/or to white matter alterations, are either not shared between them (i.e. different genetic variants affect white matter and SZ/BD risk, via separate pathways), or common in the population (i.e. have not been detected by GWAS SNP-based outputs). If the later, alternative genotyping methods, e.g. sequencing, or statistical methods, e.g. incorporating rare variants such as copy number variants in the PRS, may be necessary.

Lastly, our null hypothesis could also be harder to reject if there is a higher association of MD/FA white matter changes with positive symptoms in SZ, and of the PGC2-SZ PRS with negative symptoms. Indeed, white matter FA reductions have been associated with positive symptoms' decrease after antipsychotics, at least in fronto-temporolimbic regions (Cho et al., 2018); and the PRS (as herein, based on PGC2 variants) has been associated specifically with negative symptoms as blunted affect and emotional withdrawal (Fanous et al., 2012; Jones et al., 2016). In conclusion, our findings suggest we cannot exclude the null hypothesis that the PGC2-SZ PRS does not explain brain FA or MD variability in healthy, SZ, BD or their relatives' populations. Although a higher PRS for SZ may lead to impaired white matter integrity and poorer neural connectivity, the present test would need to be replicated in a more powerful sample, so the detected trends are confirmed.

Figure 1 - Box plot of the participants' polygenetic risk score (PRS) per diagnostic group: schizophrenia (SZ), bipolar disorder (BD), relatives (REL) of SZ or BD, and healthy controls (HC).

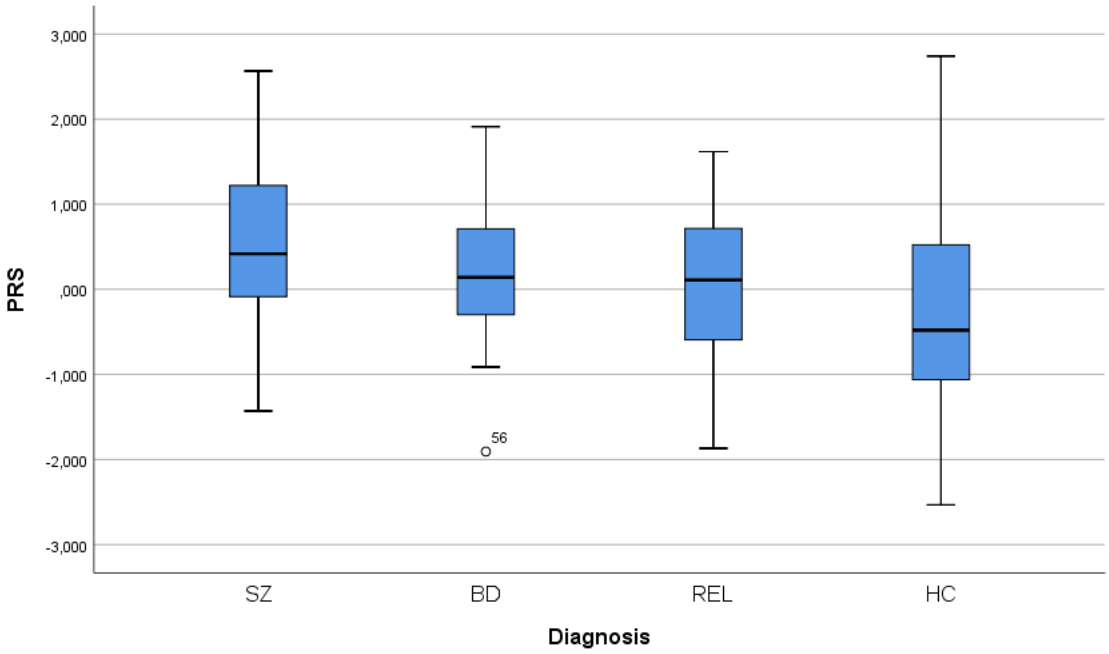

Figure 2 – Visual representation of the trend-level main effects of PRS on FA for a TFCE-uncorrected p-value < 0.01. The regions that correspond to positive effects are presented in red and the regions of the negative effects are presented in blue. The color bars represent the different 1-(p-value) in several shades of blue and red.

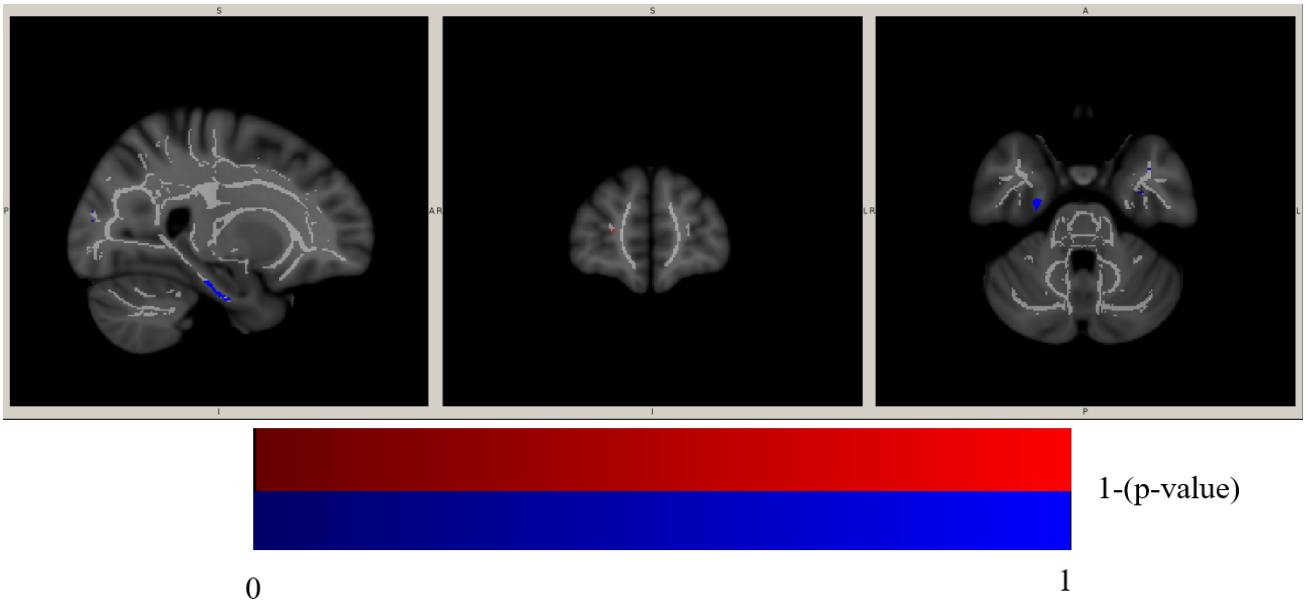

Figure 3 – Visual representation of the trend-level main effects of PRS on MD for a TFCE-uncorrected p-value < 0.01. The regions that correspond to positive effects are presented in red and the regions of the negative effects are presented in blue. The color bars represent the different 1-(p-value) in several shades of blue and red.

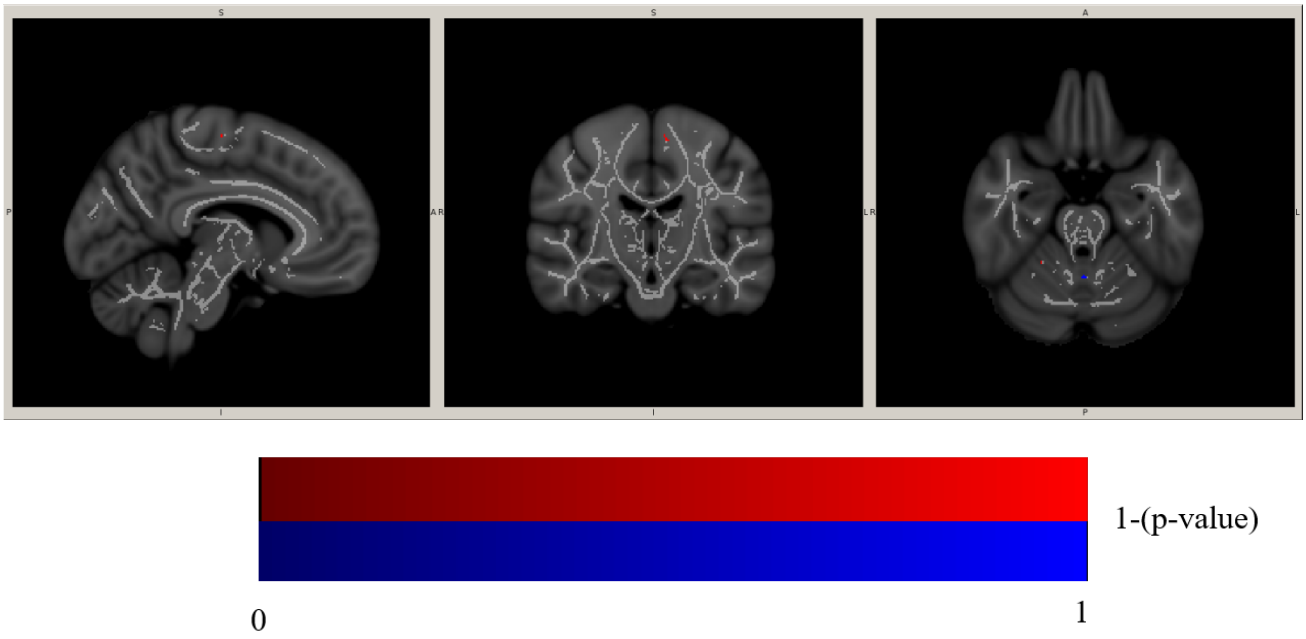

Table 1 - TFCE-uncorrected main effects of PGC2-SZ PRS on fractional anisotropy (FA) and mean diffusivity (MD), proxies of white matter microstructure, characterized in terms of cluster extent (k) (and in descending order by it), t-statistic, p-value, effect size (R^2), MNI coordinates and white matter label (R-right; L-left). PGC2-SZ PRS by Diagnosis interactions are reported in Supplementary Table 2.

Cluster extent (k)	t-statistic	p-value	R^2	Peak MNI coordinates			Cluster Label
				x{mm}	white matter{mm}	z{mm}	
Main effect of SZ PRS on FA							
Positive correlation							
3	2.239	0.007	0.035	68	182	79	Anterior thalamic radiation R
Negative correlation							
140	0.598	0.003	0.003	65	113	41	Cingulum R
50	1.649	0.004	0.019	44	70	78	Inferior longitudinal fasciculus R
36	1.747	0.006	0.022	79	109	140	Corpus callosum R
23	1.507	0.007	0.016	106	48	81	Cingulum L
23	2.016	0.005	0.029	36	80	58	Stria terminalis R
23	0.71	0.005	0.004	133	60	93	Superior longitudinal fasciculus L
23	1.215	0.006	0.011	53	48	95	Inferior longitudinal fasciculus R

16	1.017	0.005	0.007	73	117	137	Corpus callosum R
15	1.349	0.006	0.013	81	49	93	Cingulum R
12	1.423	0.008	0.015	39	75	68	Superior longitudinal fasciculus R
12	2.377	0.006	0.04	58	122	97	Superior longitudinal fasciculus R
Main effect of SZ PRS on MD							
Positive correlation							
5	2.982	0.001	0.061	97	109	133	Corticopontine tract L
4	2.735	0.005	0.052	66	80	48	Middle cerebellar peduncle R
1	2.374	0.01	0.04	118	167	65	Inferior fronto-occipital fasciculus L
1	2.873	0.002	0.057	67	84	105	Posterior corona radiata R
Negative correlation							
12	2.857	0.002	0.056	90	73	48	Inferior cerebellar peduncle

Acknowledgements

This study represents independent research part funded by the National Institute for Health Research (NIHR) Biomedical Research Centre at South London and Maudsley NHS Foundation Trust and King's College London. The views expressed are those of the authors and not necessarily those of the NHS, the NIHR or the Department of Health. DP was supported, during data collection, by Fundação para a Ciência e Tecnologia (FCT) fellowship SFRH/BD/12394/2003 and National Institute for Health Research (NIHR) grant PDF-2010-03-047, and during analysis and write-up, by an European Commission Marie Curie Career Integration grant (FP7-PEOPLE-2013-CIG-631952), FCT grants IF/00787/2014, LISBOA-01-0145-FEDER-030907 and DSAIPA/DS/0065/2018, an iMM Lisboa Director's Fund Breakthrough Idea Grant (2016), and the Bial Foundation Psychophysiology Grant (2016, Ref. 292/16)), and is co-founder of NeuroPsyAI, Ltd. None of the authors declare any conflict of interest.

Author Contributions

BS ran the neuroimaging and statistical analysis and drafted the manuscript; DP acquired some of the genetic data, revised and co-wrote the manuscript, designed and supervised the overall work, EV and

EB provided the PRS; SS, CM, TT, SK and FK provided the imaging data, RM supervised genetic and neuroimaging data collection, HF co-supervised the neuroimaging analysis.

REFERENCES

Allin, M.P., Kontis, D., Walshe, M., Wyatt, J., Barker, G.J., Kanaan, R.A., McGuire, P., Rifkin, L., Murray, R.M., Nosarti, C., 2011. White matter and cognition in adults who were born preterm. PLoS One 6, e24525. doi:10.1371/journal.pone.0024525

Ambrosi, E., Rossi-Espagnet, M.C., Kotzalidis, G.D., Comparelli, A., Del Casale, A., Carducci, F., Romano, A., Manfredi, G., Tatarelli, R., Bozzao, A., Girardi, P., 2013. Structural brain alterations in bipolar disorder II: a combined voxel-based morphometry (VBM) and diffusion tensor imaging (DTI) study. J Affect Disord 150, 610–615. doi:10.1016/j.jad.2013.02.023

Chaddock, C.A., Barker, G.J., Marshall, N., Schulze, K., Hall, M.H., Fern, A., Walshe, M., Bramon, E., Chitnis, X.A., Murray, R., McDonald, C., 2009. White matter microstructural impairments and genetic liability to familial bipolar I disorder. Br J Psychiatry 194, 527–534. doi:10.1192/bjp.bp.107.047498

Cho, S.J., Kim, M.-K., Bang, S.Y., Bang, M., Lee, S.-H., 2018. White matter integrity associated with severity reductions in positive symptoms after amisulpride treatment in drug-free patients with schizophrenia. Neurosci. Lett. 685, 131–136. doi:10.1016/j.neulet.2018.08.036

Craddock, N., Owen, M.J., 2005. The beginning of the end for the Kraepelinian dichotomy. Br. J. Psychiatry 186, 364–366. doi:10.1192/bjp.186.5.364

Ellison-Wright, I., Bullmore, E., 2009. Meta-analysis of diffusion tensor imaging studies in schizophrenia. Schizophr. Res. 108, 3–10. doi:10.1016/j.schres.2008.11.021

Fanous, A.H., Zhou, B., Aggen, S.H., Bergen, S.E., Amdur, R.L., Duan, J., Sanders, A.R., Shi, J., Mowry, B.J., Olincy, A., Amin, F., Cloninger, C.R., Silverman, J.M., Buccola, N.G., Byerley, W.F., Black, D.W., Freedman, R., Dudbridge, F., Holmans, P.A., Ripke, S., Gejman, P. V, Kendler, K.S., Levinson, D.F., 2012. Genome-wide association study of clinical dimensions of

schizophrenia: polygenic effect on disorganized symptoms. Am J Psychiatry 169, 1309–1317. doi:10.1176/appi.ajp.2012.12020218

Gurung, R., Prata, D.P., 2015. What is the impact of genome-wide supported risk variants for schizophrenia and bipolar disorder on brain structure and function? A systematic review. Psychol. Med. 45. doi:10.1017/S0033291715000537

Hummer, T.A., Francis, M.M., Vohs, J.L., Liffick, E., Mehdiyoun, N.F., Breier, A., 2016. Characterization of white matter abnormalities in early-stage schizophrenia. Early Interv Psychiatry. doi:10.1111/eip.12359

Iacono, W.G., 2018. Endophenotypes in psychiatric disease: prospects and challenges. Genome Med. 10, 11. doi:10.1186/s13073-018-0526-5

IBM Corp., 2017. IBM SPSS Statistics for Windows.

Jenkinson, M., Beckmann, C.F., Behrens, T.E., Woolrich, M.W., Smith, S.M., 2012. FSL. Neuroimage 62, 782–790. doi:10.1016/j.neuroimage.2011.09.015

Jones, H.J., Stergiakouli, E., Tansey, K.E., Hubbard, L., Heron, J., Cannon, M., Holmans, P., Lewis, G., Linden, D.E., Jones, P.B., Davey Smith, G., O'Donovan, M.C., Owen, M.J., Walters, J.T., Zammit, S., 2016. Phenotypic Manifestation of Genetic Risk for Schizophrenia During Adolescence in the General Population. JAMA Psychiatry 73, 221–228. doi:10.1001/jamapsychiatry.2015.3058

Kanaan, R., Barker, G., Brammer, M., Giampietro, V., Shergill, S., Woolley, J., Picchioni, M., Toulopoulou, T., McGuire, P., 2009. White matter microstructure in schizophrenia: Effects of disorder, duration and medication. Br. J. Psychiatry. doi:10.1192/bjp.bp.108.054320

Kanaan, R.A., Picchioni, M.M., McDonald, C., Shergill, S.S., McGuire, P.K., 2017. White matter deficits in schizophrenia are global and don't progress with age. Aust N Z J Psychiatry 51, 1020–1031. doi:10.1177/0004867417700729

Knochel, C., O'Dwyer, L., Alves, G., Reinke, B., Magerkurth, J., Rotarska-Jagiela, A., Prvulovic, D., Hampel, H., Linden, D.E.J., Oertel-Knochel, V., 2012. Association between white matter fiber integrity and subclinical psychotic symptoms in schizophrenia patients and unaffected relatives.

Schizophr. Res. 140, 129–135. doi:10.1016/j.schres.2012.06.001

Kyriakopoulos, M., Perez-Iglesias, R., Woolley, J.B., Kanaan, R.A., Vyas, N.S., Barker, G.J., Frangou, S., McGuire, P.K., 2009. Effect of age at onset of schizophrenia on white matter abnormalities. Br J Psychiatry 195, 346–353. doi:10.1192/bjp.bp.108.055376

Lener, M.S., Wong, E., Tang, C.Y., Byne, W., Goldstein, K.E., Blair, N.J., Haznedar, M.M., New, A.S., Chemerinski, E., Chu, K.-W., Rimsky, L.S., Siever, L.J., Koenigsberg, H.W., Hazlett, E.A., 2015. White matter abnormalities in schizophrenia and schizotypal personality disorder. Schizophr. Bull. 41, 300–310. doi:10.1093/schbul/sbu093

Mallas, E.-J., Carletti, F., Chaddock, C.A., Woolley, J., Picchioni, M.M., Shergill, S.S., Kane, F., Allin, M.P.G., Barker, G.J., Prata, D.P., 2016. Genome-wide discovered psychosis-risk gene ZNF804A impacts on white matter microstructure in health, schizophrenia and bipolar disorder. PeerJ 2016. doi:10.7717/peerj.1570

Mori, S., Wakana, S., van Zijl, P., Nagae-Poetcher, L.M., 2005. MRI Atlas of Human White Matter, 1st ed. Elsevier Science.

Picchioni, M.M., Toulopoulou, T., Landau, S., Davies, N., Ribchester, T., Murray, R.M., 2006. Neurological abnormalities in schizophrenic twins. Biol Psychiatry 59, 341–348. doi:10.1016/j.biopsych.2005.07.007

Prata, D., Mechelli, A., Kapur, S., 2014. Clinically meaningful biomarkers for psychosis: A systematic and quantitative review. Neurosci. Biobehav. Rev. doi:10.1016/j.neubiorev.2014.05.010

Reus, L.M., Shen, X., Gibson, J., Wigmore, E., Ligthart, L., Adams, M.J., Davies, G., Cox, S.R., Hagenaars, S.P., Bastin, M.E., Deary, I.J., Whalley, H.C., McIntosh, A.M., 2017. Association of polygenic risk for major psychiatric illness with subcortical volumes and white matter integrity in UK Biobank. Sci. Rep. 7, 42140. doi:10.1038/srep42140

Ripke, S., Neale, B.M., Corvin, A., Walters, J.T.R., Farh, K.H., Holmans, P.A., Lee, P., Bulik-Sullivan, B., Collier, D.A., Huang, H., Pers, T.H., Agartz, I., Agerbo, E., Albus, M., Alexander, M., Amin, F., Bacanu, S.A., Begemann, M., Belliveau, R.A., Bene, J., Bergen, S.E., Bevilacqua, E., Bigdeli, T.B., Black, D.W., Bruggeman, R., Buccola, N.G., Buckner, R.L.,

Byerley, W., Cahn, W., Cai, G., Campion, D., Cantor, R.M., Carr, V.J., Carrera, N., Catts, S. V., Chambert, K.D., Chan, R.C.K., Chen, R.Y.L., Chen, E.Y.H., Cheng, W., Cheung, E.F.C., Chong, S.A., Cloninger, C.R., Cohen, D., Cohen, N., Cormican, P., Craddock, N., Crowley, J.J., Curtis, D., Davidson, M., Davis, K.L., Degenhardt, F., Del Favero, J., Demontis, D., Dikeos, D., Dinan, T., Djurovic, S., Donohoe, G., Drapeau, E., Duan, J., Dudbridge, F., Durmishi, N., Eichhammer, P., Eriksson, J., Escott-Price, V., Essioux, L., Fanous, A.H., Farrell, M.S., Frank, J., Franke, L., Freedman, R., Freimer, N.B., Friedl, M., Friedman, J.I., Fromer, M., Genovese, G., Georgieva, L., Giegling, I., Giusti-Rodríguez, P., Godard, S., Goldstein, J.I., Golimbet, V., Gopal, S., Gratten, J., De Haan, L., Hammer, C., Hamshere, M.L., Hansen, M., Hansen, T., Haroutunian, V., Hartmann, A.M., Henskens, F.A., Herms, S., Hirschhorn, J.N., Hoffmann, P., Hofman, A., Hollegaard, M. V., Hougaard, D.M., Ikeda, M., Joa, I., Julià, A., Kahn, R.S., Kalaydjieva, L., Karachanak-Yankova, S., Karjalainen, J., Kavanagh, D., Keller, M.C., Kennedy, J.L., Khrunin, A., Kim, Y., Klovins, J., Knowles, J.A., Konte, B., Kucinskas, V., Kucinskiene, Z.A., Kuzelova-Ptackova, H., Kähler, A.K., Laurent, C., Keong, J.L.C., Lee, S.H., Legge, S.E., Lerer, B., Li, M., Li, T., Liang, K.Y., Lieberman, J., Limborska, S., Loughland, C.M., Lubinski, J., Lönnqvist, J., Macek, M., Magnusson, P.K.E., Maher, B.S., Maier, W., Mallet, J., Marsal, S., Mattheisen, M., Mattingsdal, M., McCarley, R.W., McDonald, C., McIntosh, A.M., Meier, S., Meijer, C.J., Melegh, B., Melle, I., Mesholam-Gately, R.I., Metspalu, A., Michie, P.T., Milani, L., Milanova, V., Mokrab, Y., Morris, D.W., Mors, O., Murphy, K.C., Murray, R.M., Myin-Germeys, I., Müller-Myhsok, B., Nelis, M., Nenadic, I., Nertney, D.A., Nestadt, G., Nicodemus, K.K., Nikitina-Zake, L., Nisenbaum, L., Nordin, A., O'Callaghan, E., O'Dushlaine, C., O'Neill, F.A., Oh, S.Y., Olincy, A., Olsen, L., Van Os, J., Pantelis, C., Papadimitriou, G.N., Papiol, S., Parkhomenko, E., Pato, M.T., Paunio, T., Pejovic-Milovancevic, M., Perkins, D.O., Pietiläinen, O., Pimm, J., Pocklington, A.J., Powell, J., Price, A., Pulver, A.E., Purcell, S.M., Quested, D., Rasmussen, H.B., Reichenberg, A., Reimers, M.A., Richards, A.L., Roffman, J.L., Roussos, P., Ruderfer, D.M., Salomaa, V., Sanders, A.R., Schall, U., Schubert, C.R., Schulze, T.G., Schwab, S.G., Scolnick, E.M., Scott, R.J., Seidman, L.J., Shi, J., Sigurdsson, E., Silagadze, T., Silverman, J.M., Sim, K., Slominsky, P., Smoller, J.W., So, H.C., Spencer, C.C.A., Stahl, E.A., Stefansson, H., Steinberg, S., Stogmann, E., Straub, R.E., Strengman, E., Strohmaier, J., Stroup, T.S., Subramaniam, M., Suvisaari, J., Svrakic, D.M., Szatkiewicz, J.P., Söderman, E., Thirumalai, S., Toncheva, D., Tosato, S., Veijola, J., Waddington, J., Walsh, D., Wang, D., Wang, Q., Webb, B.T., Weiser, M., Wildenauer, D.B., Williams, N.M., Williams, S., Witt, S.H., Wolen, A.R., Wong, E.H.M., Wormley, B.K., Xi, H.S., Zai, C.C., Zheng, X., Zimprich, F., Wray, N.R., Stefansson, K., Visscher, P.M.,

Adolfsson, R., Andreassen, O.A., Blackwood, D.H.R., Bramon, E., Buxbaum, J.D., Børglum, A.D., Cichon, S., Darvasi, A., Domenici, E., Ehrenreich, H., Esko, T., Gejman, P. V., Gill, M., Gurling, H., Hultman, C.M., Iwata, N., Jablensky, A. V., Jönsson, E.G., Kendler, K.S., Kirov, G., Knight, J., Lencz, T., Levinson, D.F., Li, Q.S., Liu, J., Malhotra, A.K., McCarroll, S.A., McQuillin, A., Moran, J.L., Mortensen, P.B., Mowry, B.J., Nöthen, M.M., Ophoff, R.A., Owen, M.J., Palotie, A., Pato, C.N., Petryshen, T.L., Posthuma, D., Rietschel, M., Riley, B.P., Rujescu, D., Sham, P.C., Sklar, P., St Clair, D., Weinberger, D.R., Wendland, J.R., Werge, T., Daly, M.J., Sullivan, P.F., O'Donovan, M.C., 2014. Biological insights from 108 schizophrenia-associated genetic loci. Nature 511, 421–427. doi:10.1038/nature13595

Ruderfer, D.M., Fanous, A.H., Ripke, S., McQuillin, A., Amdur, R.L., Gejman, P. V, O'Donovan, M.C., Andreassen, O.A., Djurovic, S., Hultman, C.M., Kelsoe, J.R., Jamain, S., Landen, M., Leboyer, M., Nimgaonkar, V., Nurnberger, J., Smoller, J.W., Craddock, N., Corvin, A., Sullivan, P.F., Holmans, P., Sklar, P., Kendler, K.S., 2014. Polygenic dissection of diagnosis and clinical dimensions of bipolar disorder and schizophrenia. Mol Psychiatry 19, 1017–1024. doi:10.1038/mp.2013.138

Shergill, S.S., Kanaan, R.A., Chitnis, X.A., O'Daly, O., Jones, D.K., Frangou, S., Williams, S.C., Howard, R.J., Barker, G.J., Murray, R.M., McGuire, P., 2007. A diffusion tensor imaging study of fasciculi in schizophrenia. Am J Psychiatry 164, 467–473. doi:10.1176/ajp.2007.164.3.467

Smith, S.M., Jenkinson, M., Johansen-Berg, H., Rueckert, D., Nichols, T.E., Mackay, C.E., Watkins, K.E., Ciccarelli, O., Cader, M.Z., Matthews, P.M., Behrens, T.E., 2006. Tract-based spatial statistics: voxelwise analysis of multi-subject diffusion data. Neuroimage 31, 1487–1505. doi:10.1016/j.neuroimage.2006.02.024

Smith, S.M., Nichols, T.E., 2009. Threshold-free cluster enhancement: addressing problems of smoothing, threshold dependence and localisation in cluster inference. Neuroimage 44, 83–98. doi:10.1016/j.neuroimage.2008.03.061

Squarcina, L., Bellani, M., Rossetti, M.G., Perlini, C., Delvecchio, G., Dusi, N., Barillari, M., Ruggeri, M., Altamura, C.A., Bertoldo, A., Brambilla, P., 2017. Similar white matter changes in schizophrenia and bipolar disorder: A tract-based spatial statistics study. PLoS One 12, e0178089. doi:10.1371/journal.pone.0178089

Subramaniam, K., Gill, J., Fisher, M., Mukherjee, P., Nagarajan, S., Vinogradov, S., 2017. White matter microstructure predicts cognitive training-induced improvements in attention and executive functioning in schizophrenia. Schizophr Res. doi:10.1016/j.schres.2017.06.062

Tesli, M., Espeseth, T., Bettella, F., Mattingsdal, M., Aas, M., Melle, I., Djurovic, S., Andreassen, O.A., 2014. Polygenic risk score and the psychosis continuum model. Acta Psychiatr Scand 130, 311–317. doi:10.1111/acps.12307

Toulopoulou, T., Zhang, X., Cherny, S., Dickinson, D., Berman, K.F., Straub, R.E., Sham, P., Weinberger, D.R., 2019. Polygenic risk score increases schizophrenia liability through cognition-relevant pathways. Brain. doi:10.1093/brain/awy279

Vassos, E., Di Forti, M., Coleman, J., Iyegbe, C., Prata, D., Euesden, J., O'Reilly, P., Curtis, C., Kolliakou, A., Patel, H., Newhouse, S., Traylor, M., Ajnakina, O., Mondelli, V., Marques, T.R., Gardner-Sood, P., Aitchison, K.J., Powell, J., Atakan, Z., Greenwood, K.E., Smith, S., Ismail, K., Pariante, C., Gaughran, F., Dazzan, P., Markus, H.S., David, A.S., Lewis, C.M., Murray, R.M., Breen, G., 2017. An Examination of Polygenic Score Risk Prediction in Individuals With First-Episode Psychosis. Biol. Psychiatry 81. doi:10.1016/j.biopsych.2016.06.028

Viher, P. V, Stegmayer, K., Giezendanner, S., Federspiel, A., Bohlhalter, S., Vanbellingen, T., Wiest, R., Strik, W., Walther, S., 2016. Cerebral white matter structure is associated with DSM-5 schizophrenia symptom dimensions. Neuroimage Clin 12, 93–99. doi:10.1016/j.nicl.2016.06.013

Vuoksimaa, E., Panizzon, M.S., Hagler, D.J., Hatton, S.N., Fennema-Notestine, C., Rinker, D., Eyler, L.T., Franz, C.E., Lyons, M.J., Neale, M.C., Tsuang, M.T., Dale, A.M., Kremen, W.S., 2017. Heritability of white matter microstructure in late middle age: A twin study of tract-based fractional anisotropy and absolute diffusivity indices. Hum. Brain Mapp. doi:10.1002/hbm.23502

Wang, Q., Cheung, C., Deng, W., Li, M., Huang, C., Ma, X., Wang, Y., Jiang, L., Sham, P.C., Collier, D.A., Gong, Q., Chua, S.E., McAlonan, G.M., Li, T., 2013. White-matter microstructure in previously drug-naive patients with schizophrenia after 6 weeks of treatment. Psychol. Med. doi:10.1017/S0033291713000238

Whalley, H.C., Sprooten, E., Hackett, S., Hall, L., Blackwood, D.H., Glahn, D.C., Bastin, M., Hall,

J., Lawrie, S.M., Sussmann, J.E., McIntosh, A.M., 2013. Polygenic risk and white matter integrity in individuals at high risk of mood disorder. Biol. Psychiatry 74, 280–286. doi:10.1016/j.biopsych.2013.01.027

Zhuo, C., Ma, X., Qu, H., Wang, L., Jia, F., Wang, C., 2016. Schizophrenia Patients Demonstrate Both Inter-Voxel Level and Intra-Voxel Level White Matter Alterations. PLoS One 11, e0162656. doi:10.1371/journal.pone.0162656

Conflict of Interest

This study represents independent research part funded by the National Institute for Health Research (NIHR) Biomedical Research Centre at South London and Maudsley NHS Foundation Trust and King's College London. The views expressed are those of the authors and not necessarily those of the NHS, the NIHR or the Department of Health. DP was supported, during data collection, by Fundação para a Ciência e Tecnologia (FCT) fellowship SFRH/BD/12394/2003 and National Institute for Health Research (NIHR) grant PDF-2010-03-047, and during analysis and write-up, by an European Commission Marie Curie Career Integration grant (FP7-PEOPLE-2013-CIG-631952), FCT grants IF/00787/2014, LISBOA-01-0145-FEDER-030907 and DSAIPA/DS/0065/2018, an iMM Lisboa Director's Fund Breakthrough Idea Grant (2016), and the Bial Foundation Psychophysiology Grant (2016), and is co-founder of NeuroPsyAI, Ltd. None of the authors declare any conflict of interest.

Author Contributions

BS ran the neuroimaging and statistical analysis and drafted the manuscript; DP acquired some of the genetic data, revised and co-wrote the manuscript, designed and supervised the overall work, EV and EB provided the PRS; SS, CM, TT, SK and FK provided the imaging data, RM supervised genetic and neuroimaging data collection, HF co-supervised the neuroimaging analysis.

Supplementary Material

EXTENDED METHODS

Participants and demographics

One hundred and fifty nine subjects who had provided DTI and PRS data were selected from a dataset used in previous studies (Picchioni *et al.*, 2006; Shergill *et al.*, 2007; Chaddock *et al.*, 2009; Kyriakopoulos *et al.*, 2009; Allin *et al.*, 2011; Mallas *et al.*, 2016; Kanaan *et al.*, 2017) at the Institute of Psychiatry, Psychology and Neuroscience (IoPPN), King's College London, with 5 subjects, across diagnostic groups, being excluded due to DTI image corruption. The remain subjects were divided in four diagnostic groups and related subjects inside the same diagnostic group were excluded to guarantee that all subjects included in the same diagnostic group were genetically independent from each other. This selection resulted in 141 subjects: SZ (n=21), BD (n=25), REL (n=27) and HC (n=68).

Statistical tests were performed using IBM SPSS statistics 25 (IBM Corp., 2017) to test if the demographic variables [age, gender, intelligence quotient (IQ), handedness and years of education (YE)] were significantly different between diagnostic groups. Kruskal-Wallis test was used for continuous demographic variables and if there were significant differences post-hoc Mann-Whitney U tests were performed. For categorical variables frequency tables were constructed to determine the Pearson Chi-Squared (χ^2). Results showed that the groups differed significantly in terms of age (Kruskal-Wallis H = 8.983; p-value =0.030) and IQ (H= 13.086; p-value = 0.004). Post-hoc tests showed that the differences in age were significant between BD and HC (Mann -Whitney U= 528.500, p-value= 0.005). Regarding IQ, significant differences were found between SZ and REL (U= 145.500; p-value= 0.004), REL and HC (U= 561.000; p-value= 0.003). Detailed results are presented in Supplementary Table 1.

PRS was not significantly associated with any of the demographic variables. However, significant differences between diagnostic groups in terms of PRSs were found, as expected (F=4.575, p-value= 0.004). Post-hoc tests revealed that the PRS for SZ was significantly higher than the PRSs in HC group (Tukey's HSD mean difference, p-value= 0.003). Detailed results are presented in Figure 1.

Supplementary Table 2 –Participants demographic data presented as mean (standard deviation) and statistical results presented as df; p-value.

Demographic Variables	SZ (n=21)	BD (n=25)	REL (n= 27)	HC (n=68)	Statistics, df, p-value
Age (years)	40.05 (2.84)	44.04 (2.33)	40.04 (2.38)	35.69 (1.68)	H= 8.983; p=0.030
IQ (z-scores)	-0.43 (0.23)	0.08 (0.25)	0.54 (0.18)	-0.08 (0.1)	H= 13.086; p=0.004
YE (years)	14.82 (0.41)	14.68 (0.68)	15.26 (0.52)	14.64 (0.30)	H=3.192; p=0.363
Gender (M/F)	15/6	10/15	13/14	34/34	??2=4.833; p=0.184
Handedness (R/L/M)	(21/0/0)	(24/0/1)	(24/3/0)	(61/5/2)	??2=6.255; p=0.395
Chlorpromazine Equivalent	218.75 (89.61)	215.00 (102.06)	-	-	-

DNA extraction and genotyping

DNA was extracted from blood or cheek swabs. The samples were genotyped at the South London and Maudsley NHS Trust/King's College London BRC Genomic Laboratory with the Illumina HumanCore Exome BeadChip. Genotypes were processed using GenomeStudio Analysis software version 2011.1 (Illumina Inc., San Diego, CA). Quality control was performed with PLINK 1.9 (https://www.cog-genomics.org/plink2). A detailed description of the genetic samples processing can be found in our previous paper (Vassos *et al.*, 2017).

Polygenetic risk score

We calculated the PRS for each participant using the PGC SZ meta-analysis (Ripke *et al.*, 2014) statistically significant SNPs, with PRSice software (http://prsice.info/). The PRSs were determined by the sum of the risk SNPs weighted by the logarithm of odds ratio of their respective association with SZ in that meta-analysis.

After the calculation of the PRS for each participant, a logistic regression was performed to analyze the association between the PRS values and the disease. This was conducted

for PRSs with different sets of thresholds (pT = 0.00000005, 0.00001, 0.0001, 0.001, 0.01, 0.05, 0.1, 0.2, 0.5, 1). The values of PRS included in this study were the ones obtained at a threshold of 0.1, because it assumes the greatest proportion of variance in case-control status explained, 9.3%, as we reported previously (Vassos *et al.*, 2017).

DTI image acquisition

MRI data was acquired using a 1.5T GE Signal LX system (General Electric, Milwaukee, WI, USA) in the Mapother House MR unit at the Maudsley Hospital, London, UK, with ~~actively shielded~~ magnetic field gradients of maximum amplitude 40 mT/m. A standard quadrature birdcage head coil was used for both radiofrequency transmission and signal reception. Diffusion data was acquired using a multi-slice peripherally-gated echo planar imaging (EPI) sequence, optimized for precise measurement of the diffusion tensor in parenchyma, from 60 contiguous near-axial slice locations for whole brain coverage, with isotropic (2.5 x 2.5 x 2.5 mm^3) resolution. At each slice location, 7 images were acquired with no diffusion gradients applied (b=0 s/mm^2), together with 64 diffusion-weighted images in which gradient directions were uniformly distributed in space. The pulse sequence parameters were chosen to provide maximum precision in the estimates of the unique elements of the diffusion tensor matrix. Further details are given elsewhere (Jones *et al.*, 2002).

Image preprocessing

Preprocessing of the diffusion MRI images was made using FMRIB software library (FSL) version 5.0.8 (Jenkinson *et al.*, 2012). The raw diffusion images were corrected for eddy currents distortions and brain-extracted to exclude non-brain voxels using the functions *eddy_correct* and *BET*, respectively. After visual inspection, the BET threshold was adjusted to 0.2 to ensure a balance between complete scalp removal and inappropriate erosion of brain tissue, not achieved with the default parameter of 0.5. FA and MD images were created by fitting a tensor model to the raw diffusion data using the FSL function *dtifit* from Functional MRI of the Brain lab (FMRIB)'s Diffusion Toolbox (FDT) within FSL.

Statistical Analysis

Voxel-wise statistical analysis of the FA data was carried out using tract-based spatial statistics (TBSS) (Smith *et al.*, 2006) in FSL. This method estimates a group *mean FA skeleton* representing the centres of all fibre bundles, across the whole brain, that are generally common to the subjects involved in the study. Each subject's FA data is then projected onto the *mean FA skeleton* in such a way that each *skeleton* voxel takes the FA value from the local center of the nearest relevant tract. The TBSS method can be divided in five steps: nonlinear alignment, identification of the target for alignment, creation of the mean FA and skeleton, projecting individual subject's FA onto the skeleton and statistics and thresholding (Smith *et al.*, 2006). To preform TBSS on FSL the functions tbss_1_preproc, tbss_2_reg, tbss_3_postreg and tbss_4_prestats were used (https://fsl.fmrib.ox.ac.uk/fsl/fslwiki/TBSS/UserGuide).

After preforming the first four steps, the data is in the form of a skeletonised 4D image, with the fourth dimension being the subject ID. In this format, the data is ready to be fed into a voxel-wise cross-subject general linear model (GLM) statistical model (Smith *et al.*, 2006). The effects of SZ PRS on FA/MD, were tested with a regression analysis, while the PRS x diagnosis interaction was tested with an ANCOVA. For this, a permutation-based approach was carried using FSL function **randomise** (https://fsl.fmrib.ox.ac.uk/fsl/fslwiki/Randomise), whereby matrices were created for the experimental design, contrasts and F-tests. The function **randomise** produces a test statistic and a threshold free cluster enhancement (TFCE)-corrected and uncorrected 1-p-value maps, for each contrast vector. This correction aims to enhance areas of signal that exhibit some spatial contiguity without relying on hard-threshold based clustering (Smith and Nichols, 2009).

To extract information about the clusters obtained after permutation inferences, the FSL function 'Cluster' was used (https://fsl.fmrib.ox.ac.uk/fsl/fslwiki/Cluster). This function returned the number of voxels of each cluster, the value of maximum "intensity" (z-statistics) inside the cluster, coordinates of the voxel with maximum "intensity" and the location of the centre of gravity (COG) within the cluster. Statistical significance was considered for TFCE-corrected results with a p-value < 0.05, while trends were considered so when showing TFCE-uncorrected results with a p-value < 0.01, following standard practice (Mallas *et al.*, 2016; Viher *et al.*, 2016; Subramaniam *et al.*, 2017). Moreover, only the 10 largest clusters of each contrast are reported, for conciseness. The

t-statistic value was extracted for every cluster peak coordinate using the fsl function **fslmeants**. For each effect, the R^2 effect size was calculated based on the t-statistics value using expression 1, where t represents the t-statistic and DF represents the degrees of freedom (subtraction of the number of variables and intercept from the number of subjects included in the analysis).

$$R^2 = \frac{t^2}{t^2 + DF} \quad (1)$$

At last, to assess the WM regions/tracts where each cluster was localized, the Johns Hopkins University ICBM-DTI-81 white-matter labels atlas was used. If cluster results were retrieved as "Unclassified", labelling was carried out manually using the MRI Atlas of Human WM (Mori *et al.*, 2005). Results were overlaid on MNI152 (1 mm) standard template and mean FA skeleton.

EXTENDED RESULTS

Supplementary Table 2 - TFCE-uncorrected SZ PRS by diagnosis interaction effects of SZ PRS on FA/MD, characterized in terms of cluster extent (k) (and in descending order by it), t-statistic, p-value, effect size at peak coordinates (R^2), MNI coordinates and WM label (R-right; L-left).

Cluster extent (k)	t-statistic	p-value	R^2	Peak MNI coordinates			Cluster Label
				x{mm}	y{mm}	z{mm}	
SZ PRS x diagnosis interaction on FA							
PRS in SZ > PRS in HC							
2	2.643	0.006	0.05	137	110	94	Superior longitudinal fasciculus L
1	2.461	0.008	0.043	131	60	99	Posterior thalamic radiation L
PRS in BD > PRS in HC							
3957	1.973	0.001	0.028	77	76	35	Middle cerebellar peduncle
416	2.57	0.002	0.047	147	86	86	Superior longitudinal fasciculus L
312	0.869	0.004	0.005	82	86	136	Corticopontine tract R
273	0.979	0.003	0.007	100	92	133	Corticopontine tract L
255	1.951	0.002	0.028	82	130	136	Corpus callosum R

246	1.674	0.002	0.02	101	51	77	Cingulum L
240	1.135	0.001	0.01	120	108	44	Cingulum L
PRS in REL > PRS in HC							
6	3.22	0.006	0.072	121	147	72	Uncinate fasciculus L
5	2.408	0.006	0.041	36	76	66	Superior longitudinal fasciculus R
1	2.416	0.009	0.041	81	108	44	Middle cerebellar peduncle
PRS in HC > PRS in SZ							
9	3.862	0	0.1	110	172	98	Corpus callosum L
3	3.137	0.002	0.068	109	69	27	Middle cerebellar peduncle
2	3.279	0.008	0.074	90	64	35	Inferior cerebellar peduncle
2	3.471	0.001	0.083	77	148	64	Uncinate fasciculus R
PRS in HC > PRS in REL							
2	2.038	0.004	0.03	108	162	110	Corticopontine tract L
1	2.732	0.01	0.053	90	64	34	Inferior cerebellar peduncle
1	2.7	0.003	0.052	123	104	106	Superior longitudinal faciculus L
PRS in BD > PRS in SZ							
1252	1.572	0.001	0.018	84	92	38	Corticopontine tract R
597	1.793	0.001	0.023	72	75	47	Middle cerebellar peduncle
525	1.8	0.002	0.024	150	100	80	Superior longitudinal fasciculus L
447	1.221	0.003	0.011	54	55	43	Inferior cerebellar peduncle
250	1.414	0.003	0.015	49	120	121	Superior longitudinal fasciculus R
194	1.405	0.002	0.015	69	85	45	Middle cerebellar peduncle
186	0.919	0.001	0.006	107	131	130	Inferior fronto-occipital fasciculus L
184	1.494	0.003	0.016	41	132	79	Superior longitudinal fasciculus R
163	1.415	0.003	0.015	83	103	75	Posterior thalamic radiation R
161	1.26	0.004	0.012	100	185	67	Corpus callosum
PRS in REL > PRS in SZ							
165	0.86	0.003	0.005	67	82	45	Middle cerebellar peduncle
6	3.045	0.001	0.064	110	172	98	Anterior thalamic radiation L
2	2.222	0.009	0.036	108	70	27	Middle cerebellar peduncle
2	3.164	0.01	0.069	72	151	122	Corticopontine tract R
1	2.472	0.008	0.044	104	146	67	Uncinate fasciculus L
1	2.877	0.009	0.058	74	79	101	Uncinate fasciculus L
1	0.86	0.003	0.005	131	60	99	Superior longitudinal fasciculus L
PRS in SZ > PRS in REL							

1	2.354	0.009	0.04	131	60	99	Superior longitudinal fasciculus L
PRS in BD > PRS in REL							
24	0.874	0.003	0.006	66	67	28	Middle cerebellar peduncle
15	0.9	0.007	0.006	78	76	36	Superior cerebellar peduncle R
14	1.195	0.006	0.011	125	117	42	Inferior longitudinal faciculus L
11	1.506	0.008	0.017	77	63	39	Anterior thalamic radiation R
9	0.5	0.008	0.002	107	131	131	Inferior fronto-occipital fasciculus L
7	2.879	0.004	0.058	57	85	113	Superior longitudinal fasciculus R
7	2.976	0.001	0.062	108	76	46	Middle cerebellar peduncle
5	2.065	0.009	0.031	72	68	36	Middle cerebellar peduncle
5	3.146	0.01	0.069	73	65	40	Middle cerebellar peduncle
4	0.842	0.009	0.005	69	58	48	Middle cerebellar peduncle
PRS in REL > PRS in BD							
1	2.556	0.007	0.046	103	36	79	Corpus callosum
1	2.608	0.005	0.048	106	54	111	Inferior longitudinal faciculus L
SZ PRS x diagnosis interaction on MD							
PRS in SZ > PRS in HC							
3	2.905	0.004	0.059	60	107	103	Superior corona radiata R
PRS in HC > PRS in SZ							
25	3.011	0.003	0.063	52	138	63	Uncinate fasciculus R
17	2.109	0.005	0.032	51	141	68	Uncinate fasciculus R
2	2.43	0.009	0.042	115	115	68	Superior longitudinal fasciculus L
2	2.904	0.008	0.059	110	178	91	Inferior fronto-occipital fasciculus L
1	2.686	0.005	0.051	64	158	104	Corpus callosum R
PRS in HC > PRS in BD							
66	1.434	0.002	0.015	108	145	124	Anterior thalamic radiation L
17	2.382	0.005	0.041	126	141	68	Uncinate fasciculus L
7	4.238	0.001	0.118	99	113	127	Corpus callosum L
5	0.733	0.007	0.004	59	76	125	Superior longitudinal fasciculus R
3	2.72	0.008	0.052	53	143	68	Uncinate fasciculus R
3	2.816	0.006	0.056	75	78	102	Cingulum R
2	1.304	0.008	0.013	94	136	49	Uncinate fasciculus L
2	2.271	0.006	0.037	99	108	66	Anterior thalamic radiation L
2	2.792	0.009	0.055	65	68	122	Inferior fronto-occipital fasciculus R
1	3.101	0.006	0.067	105	65	30	Middle cerebellar peduncle L

PRS in HC > PRS in REL							
1	1.946	0.007	0.027	80	41	89	Cingulum R
1	2.369	0.009	0.04	79	42	91	Cingulum R
PRS in SZ > PRS in BD							
5	2.454	0.003	0.043	106	68	29	Middle cerebellar peduncle
3	2.387	0.008	0.041	60	107	104	Superior corona radiata R
2	3.692	0.003	0.092	99	113	127	Corpus callosum L
PRS in REL > PRS in SZ							
18	2.359	0.005	0.04	50	136	65	Uncinate fasciculus R
6	2.093	0.003	0.032	89	69	57	Infer cerebellar peduncle
1	2.725	0.004	0.053	107	50	41	Inferior cerebellar peduncle
1	1.721	0.006	0.022	90	72	47	Inferior cerebellar peduncle
1	2.874	0.006	0.058	53	129	72	Uncinate fasciculus R
PRS in REL > PRS in BD							
2	2.534	0.004	0.046	108	50	41	Inferior cerebellar peduncle
1	2.803	0.007	0.055	105	65	30	Middle cerebellar peduncle L
1	2.438	0.009	0.042	112	99	69	Anterior thalamic radiation L
1	3.17	0.01	0.07	99	113	127	Corpus callosum L

Supplementary Table 3 – Smaller TFCE-uncorrected effects of SZ PRS on FA/MD, characterized in terms of cluster extent (k) (and in descending order by it), t-statistic, p-value, effect size (R^2), MNI coordinates and WM label (R-right; L-left).

Cluster extent (k)	**p-value**	**Peak MNI coordinates**		
		x{mm}	**y{mm}**	**z{mm}**
Main effect of SZ PRS on FA				
Negative correlation				
12	0.008	39	75	68
12	0.006	58	122	97
11	0.009	119	91	60
10	0.007	80	144	129
10	0.006	53	53	63
9	0.009	104	99	69
9	0.004	122	82	68

7	0.006	106	119	137
6	0.009	135	74	68
6	0.003	77	122	111
6	0.007	63	37	85
5	0.005	97	109	134
5	0.009	131	57	67
5	0.009	58	52	66
4	0.002	98	97	67
4	0.009	126	132	40
3	0.009	123	53	109
3	0.009	102	130	130
3	0.007	32	86	66
3	0.009	122	119	41
3	0.007	66	37	90
3	0.009	41	83	68
2	0.007	73	38	75
2	0.008	105	64	73
2	0.010	119	74	71
2	0.008	62	38	70
2	0.008	132	70	70
2	0.010	116	87	64
2	0.008	137	71	67
2	0.006	34	86	65
2	0.008	113	93	59
2	0.009	126	102	48
2	0.004	115	165	63
1	0.010	40	74	62
1	0.010	127	86	112
1	0.010	54	60	109
1	0.008	81	97	64
1	0.010	37	95	53
1	0.006	131	70	103
1	0.010	82	46	98
1	0.010	99	118	134
1	0.010	113	89	64

1	0.008	132	119	37
1	0.009	141	71	66
1	0.003	102	41	85
1	0.008	59	42	83
1	0.005	94	100	67
1	0.009	101	51	77
1	0.005	108	129	75
1	0.007	139	69	75
1	0.010	100	47	75
1	0.009	106	82	74
1	0.010	133	67	68
1	0.010	38	84	68
1	0.010	136	69	73
1	0.010	33	85	68
1	0.009	82	160	68
1	0.009	139	72	65
SZ PRS x diagnosis interaction on FA				
PRS in SZ > PRS in HC				
138	0.002	95	113	71
134	0.002	66	34	83
107	0.004	80	37	87
95	0.004	50	79	56
92	0.002	63	36	76
85	0.005	33	97	62
74	0.004	69	85	45
74	0.004	103	55	120
72	0.003	63	120	111
71	0.004	81	102	67
69	0.005	113	64	122
68	0.006	33	113	72
68	0.003	100	185	65
64	0.004	53	98	46
64	0.005	108	45	48
63	0.003	104	33	85
63	0.007	105	127	63
60	0.004	121	73	59

58	0.006	81	48	97
55	0.007	131	145	107
49	0.005	101	61	123
44	0.006	116	47	75
43	0.007	73	43	90
38	0.007	118	57	39
37	0.002	93	134	51
36	0.005	103	71	125
35	0.004	83	104	74
35	0.002	97	104	126
34	0.006	97	56	105
33	0.004	128	55	65
32	0.002	76	146	65
31	0.007	98	98	51
31	0.007	40	92	59
30	0.003	49	62	63
29	0.006	129	160	64
27	0.004	121	163	99
25	0.002	73	38	94
24	0.005	57	114	130
23	0.002	64	161	102
22	0.005	53	160	93
21	0.006	76	77	53
21	0.007	107	81	134
21	0.006	100	137	65
21	0.004	59	165	94
20	0.007	124	129	69
20	0.008	127	78	63
19	0.007	113	119	63
19	0.008	120	165	81
18	0.008	37	88	92
18	0.002	129	84	55
18	0.007	49	120	122
18	0.008	124	117	72
17	0.007	73	162	104
15	0.004	113	104	68
15	0.006	56	172	88
14	0.008	110	148	68

13	0.007	99	41	66
12	0.009	121	50	43
12	0.008	39	122	64
12	0.003	57	175	79
12	0.008	57	112	104
11	0.007	124	167	69
10	0.008	87	91	84
10	0.008	73	73	25
10	0.005	125	45	65
9	0.008	112	99	78
9	0.007	106	101	71
9	0.009	123	51	72
9	0.009	59	76	46
9	0.007	41	109	47
9	0.009	102	86	83
9	0.008	64	69	99
8	0.006	93	125	77
8	0.008	123	105	64
8	0.007	119	156	96
8	0.007	66	147	109
7	0.008	110	125	86
7	0.008	123	90	51
7	0.007	101	72	131
7	0.008	81	182	61
7	0.009	105	180	70
7	0.009	75	141	69
7	0.007	74	50	81
7	0.007	102	186	80
7	0.008	57	131	76
7	0.009	116	134	94
6	0.009	120	131	82
6	0.008	129	73	85
6	0.009	64	48	77
6	0.007	132	159	71
6	0.007	60	176	65
6	0.007	102	181	92
6	0.005	81	136	63
6	0.009	129	60	38

6	0.002	105	77	50
5	0.009	72	157	108
5	0.007	60	85	39
5	0.008	79	184	64
5	0.006	61	132	88
5	0.006	108	105	88
5	0.007	31	90	88
5	0.008	39	98	50
4	0.009	119	95	70
4	0.009	116	92	101
4	0.008	130	72	80
4	0.008	124	81	57
4	0.008	86	99	54
4	0.009	116	128	97
4	0.009	39	102	52
4	0.009	57	168	73
4	0.007	51	57	66
4	0.007	124	120	72
4	0.007	111	95	69
4	0.007	72	89	134
3	0.007	102	98	82
3	0.004	108	76	46
3	0.010	74	45	93
3	0.009	30	105	79
3	0.009	69	91	137
3	0.008	83	87	40
3	0.009	121	134	89
3	0.010	59	162	91
3	0.009	120	102	68
3	0.007	82	111	76
3	0.009	37	109	73
3	0.009	78	106	74
3	0.004	101	66	121
3	0.010	64	102	72
3	0.007	104	182	71
3	0.002	122	94	70
3	0.007	59	52	78
2	0.010	99	113	56

2	0.009	108	67	114
2	0.009	30	97	80
2	0.008	95	103	50
2	0.010	59	127	84
2	0.009	108	68	116
2	0.010	137	78	70
2	0.009	58	157	95
2	0.009	100	107	72
2	0.005	108	57	42
2	0.007	137	110	94
2	0.010	95	116	68
2	0.009	95	123	71
2	0.008	81	111	71
2	0.009	33	86	92
2	0.009	62	38	70
2	0.009	74	40	67
2	0.010	101	62	108
2	0.009	139	82	68
2	0.010	104	75	122
2	0.001	116	86	108
2	0.009	140	80	107
2	0.008	133	85	104
2	0.007	89	107	65
2	0.010	120	135	78
2	0.010	119	102	64
2	0.009	128	82	64
2	0.009	120	53	78
2	0.010	123	121	75
2	0.009	59	115	63
2	0.010	79	100	62
2	0.008	98	107	76
2	0.008	139	69	75
2	0.008	108	63	123
2	0.007	69	178	62
2	0.010	114	69	110
2	0.009	120	112	62
1	0.010	57	115	125
1	0.009	119	122	91

1	0.010	119	124	91
1	0.003	132	88	112
1	0.010	114	63	119
1	0.009	108	82	129
1	0.010	63	140	112
1	0.010	106	125	123
1	0.010	73	88	130
1	0.009	72	43	98
1	0.010	60	119	114
1	0.010	75	119	129
1	0.010	116	137	95
1	0.010	60	157	109
1	0.010	118	158	94
1	0.010	78	59	123
1	0.010	122	130	75
1	0.008	135	65	75
1	0.010	56	58	75
1	0.010	79	47	75
1	0.010	78	134	74
1	0.010	61	50	74
1	0.010	68	148	73
1	0.010	112	102	72
1	0.009	56	168	71
1	0.008	95	120	71
1	0.009	61	101	70
1	0.010	85	115	69
1	0.009	99	110	68
1	0.010	121	99	68
1	0.009	120	117	67
1	0.010	67	92	135
1	0.010	107	147	65
1	0.009	123	48	65
1	0.009	109	109	64
1	0.010	107	108	63
1	0.009	78	181	62
1	0.009	96	115	59
1	0.010	83	95	57
1	0.007	98	67	57

1	0.009	128	89	56
1	0.009	98	100	44
1	0.010	125	56	42
1	0.010	83	89	41
1	0.010	128	64	41
1	0.009	74	75	33
1	0.009	74	71	26
1	0.010	85	114	67
1	0.008	61	128	90
1	0.010	112	128	89
1	0.010	105	116	89
1	0.010	103	181	88
1	0.009	59	163	88
1	0.009	120	128	88
1	0.010	59	128	88
1	0.009	103	111	88
1	0.010	101	118	87
1	0.009	105	102	87
1	0.010	119	109	86
1	0.008	88	87	86
1	0.010	77	86	85
1	0.010	94	90	84
1	0.010	96	89	83
1	0.010	58	170	75
1	0.010	30	102	82
1	0.009	71	101	81
1	0.010	113	111	80
1	0.010	130	74	80
1	0.010	59	133	79
1	0.010	30	102	78
1	0.009	120	163	77
1	0.006	89	115	77
1	0.008	100	107	77
1	0.009	51	70	77
1	0.010	139	69	77
1	0.010	111	148	76
1	0.009	100	105	76
1	0.010	136	67	76

1	0.009	57	56	76
1	0.007	58	55	83
138	0.002	95	113	71
134	0.002	66	34	83
107	0.004	80	37	87
95	0.004	50	79	56
92	0.002	63	36	76
85	0.005	33	97	62
74	0.004	69	85	45
74	0.004	103	55	120
72	0.003	63	120	111
71	0.004	81	102	67
69	0.005	113	64	122
68	0.006	33	113	72
68	0.003	100	185	65
64	0.004	53	98	46
64	0.005	108	45	48
63	0.003	104	33	85
63	0.007	105	127	63
60	0.004	121	73	59
58	0.006	81	48	97
55	0.007	131	145	107
49	0.005	101	61	123
44	0.006	116	47	75
43	0.007	73	43	90
38	0.007	118	57	39
37	0.002	93	134	51
36	0.005	103	71	125
35	0.004	83	104	74
35	0.002	97	104	126
34	0.006	97	56	105
33	0.004	128	55	65
32	0.002	76	146	65
31	0.007	98	98	51
31	0.007	40	92	59
30	0.003	49	62	63
29	0.006	129	160	64
27	0.004	121	163	99

25	0.002	73	38	94
24	0.005	57	114	130
23	0.002	64	161	102
22	0.005	53	160	93
21	0.006	76	77	53
21	0.007	107	81	134
21	0.006	100	137	65
21	0.004	59	165	94
20	0.007	124	129	69
20	0.008	127	78	63
19	0.007	113	119	63
19	0.008	120	165	81
18	0.008	37	88	92
18	0.002	129	84	55
18	0.007	49	120	122
18	0.008	124	117	72
17	0.007	73	162	104
15	0.004	113	104	68
15	0.006	56	172	88
14	0.008	110	148	68
13	0.007	99	41	66
12	0.009	121	50	43
12	0.008	39	122	64
12	0.003	57	175	79
12	0.008	57	112	104
11	0.007	124	167	69
10	0.008	87	91	84
10	0.008	73	73	25
10	0.005	125	45	65
9	0.008	112	99	78
9	0.007	106	101	71
9	0.009	123	51	72
9	0.009	59	76	46
9	0.007	41	109	47
9	0.009	102	86	83
9	0.008	64	69	99
8	0.006	93	125	77
8	0.008	123	105	64

8	0.007	119	156	96
8	0.007	66	147	109
7	0.008	110	125	86
7	0.008	123	90	51
7	0.007	101	72	131
7	0.008	81	182	61
7	0.009	105	180	70
7	0.009	75	141	69
7	0.007	74	50	81
7	0.007	102	186	80
7	0.008	57	131	76
7	0.009	116	134	94
6	0.009	120	131	82
6	0.008	129	73	85
6	0.009	64	48	77
6	0.007	132	159	71
6	0.007	60	176	65
6	0.007	102	181	92
6	0.005	81	136	63
6	0.009	129	60	38
6	0.002	105	77	50
5	0.009	72	157	108
5	0.007	60	85	39
5	0.008	79	184	64
5	0.006	61	132	88
5	0.006	108	105	88
5	0.007	31	90	88
5	0.008	39	98	50
4	0.009	119	95	70
4	0.009	116	92	101
4	0.008	130	72	80
4	0.008	124	81	57
4	0.008	86	99	54
4	0.009	116	128	97
4	0.009	39	102	52
4	0.009	57	168	73
4	0.007	51	57	66
4	0.007	124	120	72

4	0.007	111	95	69
4	0.007	72	89	134
3	0.007	102	98	82
3	0.004	108	76	46
3	0.010	74	45	93
3	0.009	30	105	79
3	0.009	69	91	137
3	0.008	83	87	40
3	0.009	121	134	89
3	0.010	59	162	91
3	0.009	120	102	68
3	0.007	82	111	76
3	0.009	37	109	73
3	0.009	78	106	74
3	0.004	101	66	121
3	0.010	64	102	72
3	0.007	104	182	71
3	0.002	122	94	70
3	0.007	59	52	78
2	0.010	99	113	56
2	0.009	108	67	114
2	0.009	30	97	80
2	0.008	95	103	50
2	0.010	59	127	84
2	0.009	108	68	116
2	0.010	137	78	70
2	0.009	58	157	95
2	0.009	100	107	72
2	0.005	108	57	42
2	0.007	137	110	94
2	0.010	95	116	68
2	0.009	95	123	71
2	0.008	81	111	71
2	0.009	33	86	92
2	0.009	62	38	70
2	0.009	74	40	67
2	0.010	101	62	108
2	0.009	139	82	68

2	0.010	104	75	122
2	0.001	116	86	108
2	0.009	140	80	107
2	0.008	133	85	104
2	0.007	89	107	65
2	0.010	120	135	78
2	0.010	119	102	64
2	0.009	128	82	64
2	0.009	120	53	78
2	0.010	123	121	75
2	0.009	59	115	63
2	0.010	79	100	62
2	0.008	98	107	76
2	0.008	139	69	75
2	0.008	108	63	123
2	0.007	69	178	62
2	0.010	114	69	110
2	0.009	120	112	62
1	0.010	57	115	125
1	0.009	119	122	91
1	0.010	119	124	91
1	0.003	132	88	112
1	0.010	114	63	119
1	0.009	108	82	129
1	0.010	63	140	112
1	0.010	106	125	123
1	0.010	73	88	130
1	0.009	72	43	98
1	0.010	60	119	114
1	0.010	75	119	129
1	0.010	116	137	95
1	0.010	60	157	109
1	0.010	118	158	94
1	0.010	78	59	123
1	0.010	122	130	75
1	0.008	135	65	75
1	0.010	56	58	75
1	0.010	79	47	75

1	0.010	78	134	74
1	0.010	61	50	74
1	0.010	68	148	73
1	0.010	112	102	72
1	0.009	56	168	71
1	0.008	95	120	71
1	0.009	61	101	70
1	0.010	85	115	69
1	0.009	99	110	68
1	0.010	121	99	68
1	0.009	120	117	67
1	0.010	67	92	135
1	0.010	107	147	65
1	0.009	123	48	65
1	0.009	109	109	64
1	0.010	107	108	63
1	0.009	78	181	62
1	0.009	96	115	59
1	0.010	83	95	57
1	0.007	98	67	57
1	0.009	128	89	56
1	0.009	98	100	44
1	0.010	125	56	42
1	0.010	83	89	41
1	0.010	128	64	41
1	0.009	74	75	33
1	0.009	74	71	26
1	0.010	85	114	67
1	0.008	61	128	90
1	0.010	112	128	89
1	0.010	105	116	89
1	0.010	103	181	88
1	0.009	59	163	88
1	0.009	120	128	88
1	0.010	59	128	88
1	0.009	103	111	88
1	0.010	101	118	87
1	0.009	105	102	87

1	0.010	119	109	86
1	0.008	88	87	86
1	0.010	77	86	85
1	0.010	94	90	84
1	0.010	96	89	83
1	0.010	58	170	75
1	0.010	30	102	82
1	0.009	71	101	81
1	0.010	113	111	80
1	0.010	130	74	80
1	0.010	59	133	79
1	0.010	30	102	78
1	0.009	120	163	77
1	0.006	89	115	77
1	0.008	100	107	77
1	0.009	51	70	77
1	0.010	139	69	77
1	0.010	111	148	76
1	0.009	100	105	76
1	0.010	136	67	76
1	0.009	57	56	76
1	0.007	58	55	83
PRS in BD > PRS in SZ				
158	0.003	76	145	122
154	0.005	30	95	82
150	0.002	97	95	30
115	0.005	104	156	112
114	0.002	64	161	102
81	0.005	48	143	90
78	0.003	76	146	66
68	0.006	118	127	37
65	0.003	63	67	42
56	0.006	106	103	139
49	0.004	99	110	138
45	0.007	78	152	123
38	0.007	131	150	101
37	0.007	106	126	124
33	0.004	75	96	82

31	0.004	57	175	81
31	0.005	55	66	28
31	0.003	66	144	111
30	0.006	108	90	136
29	0.002	66	67	28
28	0.007	79	181	62
28	0.007	110	96	121
25	0.007	60	142	106
25	0.005	99	92	134
24	0.007	72	166	99
23	0.007	101	105	51
22	0.007	95	107	69
21	0.008	103	88	132
20	0.004	40	110	114
20	0.008	73	134	80
19	0.005	102	187	74
18	0.008	107	178	82
18	0.005	46	98	97
17	0.007	58	131	108
17	0.006	113	88	45
17	0.006	71	162	103
16	0.007	61	177	65
16	0.007	97	118	137
16	0.006	103	87	141
15	0.008	107	145	115
13	0.007	59	163	88
12	0.006	119	120	41
12	0.006	85	107	66
12	0.007	82	101	126
11	0.009	57	137	96
11	0.006	77	104	86
10	0.009	72	156	108
10	0.007	130	128	38
10	0.007	78	117	70
10	0.008	100	118	138
9	0.006	108	82	46
9	0.008	121	140	122
8	0.006	58	137	125

8	0.001	110	172	98
7	0.004	98	109	62
7	0.005	59	166	94
6	0.009	75	141	69
6	0.008	40	100	78
6	0.009	122	175	80
6	0.009	101	83	116
6	0.008	72	68	32
5	0.009	85	114	67
5	0.006	72	107	88
5	0.008	59	133	109
5	0.008	109	67	47
5	0.004	95	114	71
5	0.007	95	105	74
5	0.007	58	147	118
5	0.008	66	74	127
4	0.006	112	99	80
4	0.009	64	95	80
4	0.007	118	162	97
4	0.008	121	163	99
4	0.009	78	134	74
4	0.009	59	147	104
4	0.008	97	146	56
4	0.008	63	102	71
4	0.009	98	144	59
4	0.009	73	150	112
3	0.009	58	138	119
3	0.007	97	89	128
3	0.009	99	88	115
3	0.008	33	122	87
3	0.009	108	141	114
3	0.008	75	117	91
3	0.008	51	76	36
3	0.008	104	48	46
3	0.004	105	65	30
3	0.001	109	69	27
3	0.008	133	84	105
3	0.009	113	46	46

3	0.009	123	79	44
3	0.009	40	127	107
3	0.009	38	122	91
3	0.008	66	44	68
3	0.009	74	102	71
3	0.009	80	111	71
3	0.006	64	36	77
3	0.008	116	73	48
2	0.009	103	109	58
2	0.007	62	95	78
2	0.009	77	103	53
2	0.008	65	158	97
2	0.009	65	68	122
2	0.009	90	87	38
2	0.009	116	93	101
2	0.009	90	89	43
2	0.007	77	148	64
2	0.009	101	168	56
2	0.010	102	106	54
2	0.009	94	109	72
2	0.007	108	57	42
2	0.008	99	104	41
2	0.000	116	86	108
2	0.009	125	145	108
2	0.009	61	101	70
2	0.010	57	159	95
2	0.007	56	169	87
2	0.008	107	108	63
2	0.009	59	133	113
2	0.009	76	111	88
2	0.008	108	104	137
2	0.010	74	114	91
2	0.007	75	112	90
2	0.008	74	107	90
2	0.007	70	104	90
2	0.010	107	45	47
2	0.008	58	114	63
2	0.009	113	85	35

1	0.009	67	152	62
1	0.010	108	137	116
1	0.010	102	118	135
1	0.009	107	82	136
1	0.010	75	176	61
1	0.009	56	141	67
1	0.010	73	151	114
1	0.009	104	158	113
1	0.004	104	146	67
1	0.010	60	138	113
1	0.009	86	108	62
1	0.010	71	174	66
1	0.009	58	140	118
1	0.010	73	70	34
1	0.010	102	147	64
1	0.010	100	91	130
1	0.009	108	82	129
1	0.009	109	109	64
1	0.009	71	69	38
1	0.008	121	121	35
1	0.010	97	144	63
1	0.009	81	98	126
1	0.010	58	109	64
1	0.009	106	91	38
1	0.010	73	55	50
1	0.008	115	78	48
1	0.009	73	108	92
1	0.010	54	139	91
1	0.009	75	133	78
1	0.008	76	120	89
1	0.010	56	172	88
1	0.010	98	96	140
1	0.010	76	107	88
1	0.004	71	94	80
1	0.008	131	84	81
1	0.009	69	99	87
1	0.010	98	107	46
1	0.010	72	102	85

1	0.009	69	98	85
1	0.009	124	170	84
1	0.008	78	110	88
1	0.010	102	165	56
1	0.003	132	88	112
1	0.009	95	105	69
1	0.010	70	65	40
1	0.008	85	115	69
1	0.010	115	94	106
1	0.010	107	160	104
1	0.010	126	122	41
1	0.009	108	169	93
1	0.009	104	170	101
1	0.010	107	161	101
1	0.010	77	137	74
1	0.010	49	126	100
1	0.009	116	89	100
1	0.010	68	95	76
1	0.010	111	98	76
1	0.009	111	78	77
1	0.010	88	89	42
PRS in BD > PRS in REL				
4	0.009	124	108	43
4	0.006	78	69	29
4	0.007	118	111	41
3	0.009	78	75	39
3	0.009	121	103	43
2	0.002	116	86	108
2	0.007	105	65	30
1	0.009	80	89	33
1	0.009	82	56	44
1	0.009	72	57	46
1	0.008	87	59	46
1	0.009	71	67	33
SZ PRS x diagnosis interaction on MD				
PRS in HC > PRS in BD				
1	0.003	112	99	69
1	0.01	55	150	99

1	0.003	66	85	116
1	0.009	108	133	132

PLOTS OF MAIN RESULTS

Note: *Given that the imaging software we are using (FSL) does not provide plots for the TFCE analysis, we resorted to extracting the FA/MD values in the coordinate where the effect peaked in each cluster, and placing them in a statistics plotting-able software such as SPSS, as is often done in the literature, to aid the imaging analysis interpretation. Given that most effects we report (in Table 1) are slight trends, and the TFCE analysis employed does not only take into account the peak differences but simultaneously the voxel-wise neighborhood of these differences, the plots (below) we obtained for the peak values do not necessarily represent the TFCE-based trend (shown in Table 1).*

Supplementary Figure 3 – Correlation plot of the positive effect of the PRS on anterior thalamic radiation's FA (x, y, z: 68, 182, 79).

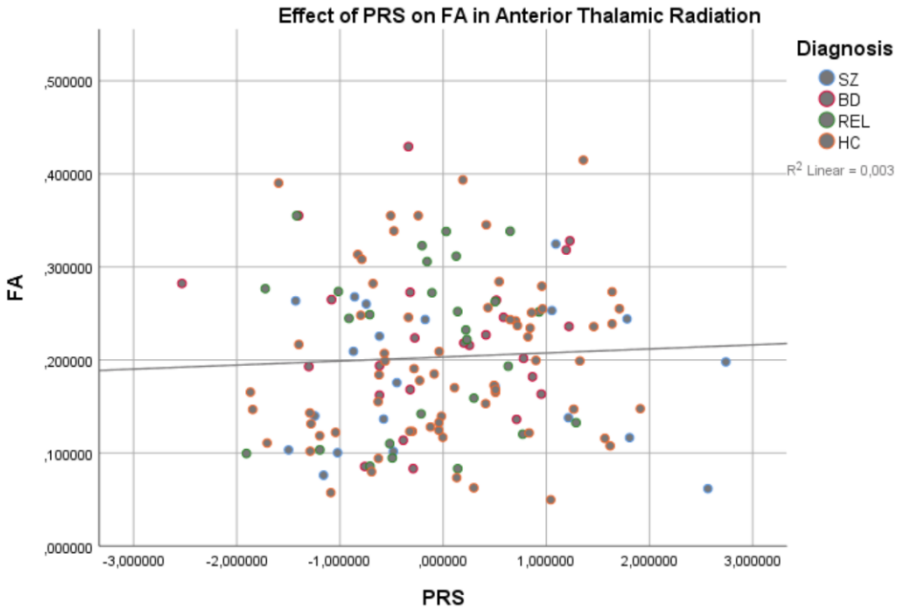

Supplementary Figure 2 – Correlation plot of the negative effect of the PRS on the cingulum's FA (x, y, z: 65, 113, 41).

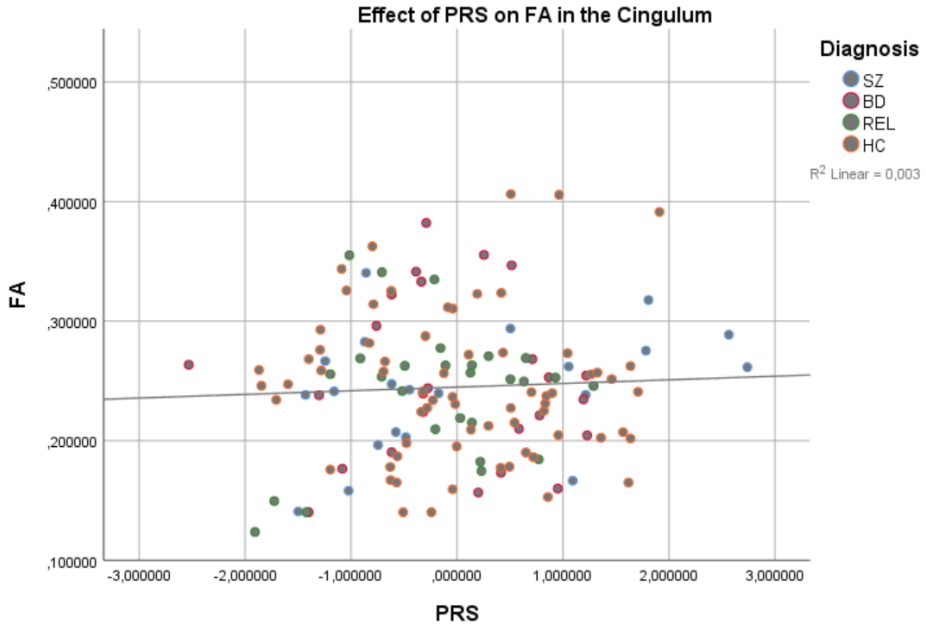

Supplementary Figure 3 – Correlation plot of the positive effect of the PRS on corticopontine tract's MD (x, y, z: 97 ,109 ,133).

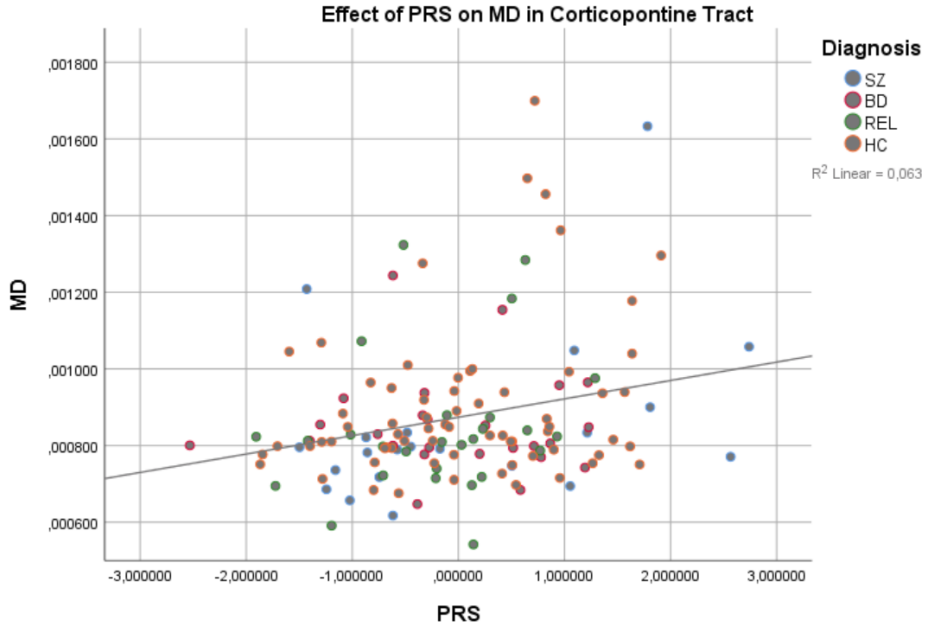

Supplementary Figure 4 – Correlation plot of the negative effect of the PRS on inferior cerebellar peduncle's MD (x, y, z: 90, 73, 48).

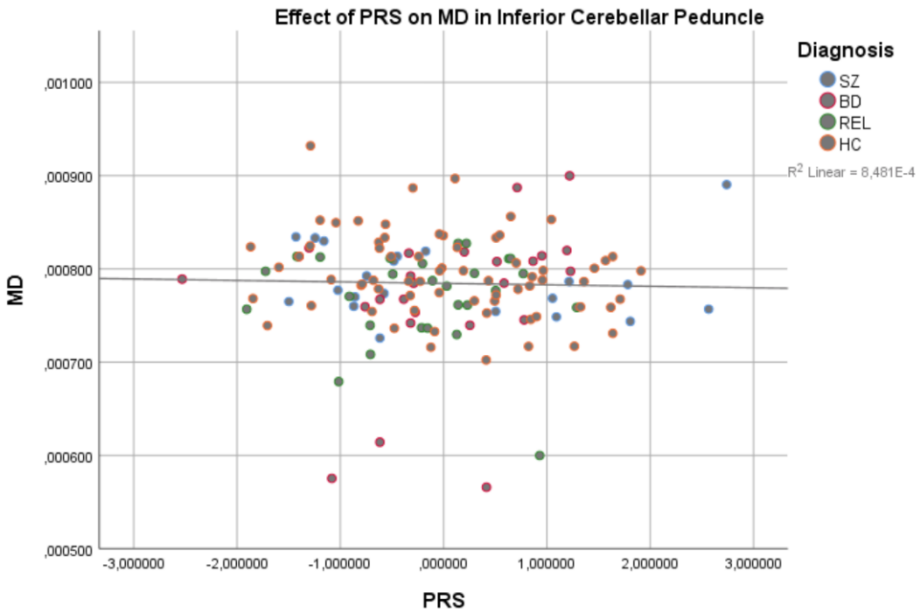
Effect of PRS on MD in Inferior Cerebellar Peduncle
Diagnosis
SZ
BD
REL
HC
R2 Linear = 8,481E-4
MD
,001000
,000900
,000800
,000700
,000600
,000500
-3,000000
-2,000000
-1,000000
,000000
1,000000
2,000000
3,000000
PRS